14th International Conference on Structural Safety and Reliability - ICOSSAR'25
1-6 June, 2025 - Los Angeles California, USA
R. Ghanem, E. Johnson, S. Masri and A. Olivier (Eds)

PROBABILISTIC DEMAND HAZARD ASSESSMENT OF A RC BUILDING WITH BUCKLING RESTRAINED BRACES EXPOSED TO SEISMIC LOADINGS

ITZEL E. RAMIREZ[1], J. RAMON GAXIOLA-CAMACHO[2] AND DANTE TOLENTINO[3]

[1] Departamento de materiales, Universidad Autónoma Metropolitana
420 San Pablo Avenue, Nueva el Rosario, Azcapotzalco, Mexico City 02128, Mexico
al2233802163@azc.uam.mx

[2] Facultad de Ingeniería, Universidad Autónoma de Sinaloa
Ciudad Universitaria, Culiacán, 80040, México
jrgaxiola@uas.edu.mx

[3] Departamento de materiales, Universidad Autónoma Metropolitana
420 San Pablo Avenue, Nueva el Rosario, Azcapotzalco, Mexico City 02128, Mexico
dantetl@azc.uam.mx

Key words: Fragility, Nonstructural elements, Buckling-restrained braces, Demand exceedance rate

Abstract. Hospitals are considered essential institutions that must continue to operate after a natural disaster or emergency. Their ability to serve users depends not only on immediate response in medical terms, but also on the capacity of their facilities to resist environmental loads. In this regard, dissipation systems have been used as a solution to improve the seismic behavior of building structures. This paper estimates demand exceedance rates of a 10-story reinforced concrete (RC) hospital building with buckling restrained braces (BRBs) located in soft soil of Mexico City. Different performance thresholds are considered to evaluate both structural fragility and demand exceedance rates of structural and non-structural elements derived from nonlinear dynamic analysis. Uncertainties associated with the occurrence of seismic loadings are considered. The use of dissipation systems could be an alternative solution to improve both structural performance and system reliability for a given environmental loading.

1 INTRODUCTION

The functionality of hospitals during and after a major earthquake is critical, not only to ensure patient safety, but also to enable effective emergency response. Although significant attention is focused on structural integrity, the proper functionality depends on the condition of non-structural elements such as ventilators, X-ray equipment, intensive care monitors, operating tables, among others. On the other hand, the process of restoring operations or information after a strong earthquake could be a challenging task as most of the damaged components take a long time. Mexico City is considered an area of high seismicity due to historical seismic events such as the 1985 and 2017 earthquakes, which demonstrated the vulnerability of hospital infrastructure. Although the structural damage has been reduced, there

are still concerns about the nonstructural elements and contents, especially in hospitals that must remain at operational levels during and after an earthquake. Therefore, there is a need to improve seismic design, not only on the structural elements but also on the non-structural components in important structures such as hospitals. Based on the above, different studies have been estimated the seismic fragility such as Rossetto [1] that propose a method to estimate analytical fragility curves in RC structures considering uncertainties in material and ground motions. Ranjbar [2] evaluate the seismic fragility buildings to assess the potential damage during a during an earthquake. Herrera and Tolentino [3] estimate structural fragility in RC structures considering seismic loads and corrosion in time. Hospital buildings are important for society, especially when a strong earthquake occurs then, many studies have been calculated fragility functions of hospitals such as Shooraki et al. [4] that determine fragility curves for low and mid-rise of both RC and masonry hospital buildings. Gubana and Mazelli [5] establish comprehensive fragility curves for a complex RC hospitals. Non-structural components are not part of a structural member that resists lateral loads, but their failure can affect significantly the operability of a hospital building. Moreover, the repair cost of the non-structural members represents a significant percentage of the repair cost [6].

The BRBs have demonstrated an efficient cost-benefit solution to limit the lateral displacement and offers to resist both tension and compression forces. This type of devices have been studied in literature as Hu et al. [7] that investigate how the brace configuration and building height affect the seismic performance of BRBs using a probabilistic seismic assessment. Maulana et al. [8] determine the optimal number and location of BRBS in a RC structure with shear walls using a genetic algorithm. Suzuki et al. [9] quantify the risk across different seismic regions of a RC structure with BRBs.

2 PROBABILISTIC EXCEEDANCE DEMAND RATES

The exceedance demand rate, $\nu_D(d)$, can be estimated as follows [10]: [10]

$$\nu_D(d) = \int_0^\infty \nu_D(y) P(D \geq d|y)\, dy \tag{1}$$

where $\nu_D(y)$ represent the first derivate of the seismic hazard curve; $P(D \geq d|y)$ is the probability that demand D exceeds a preestablished damage threshold d, for a given intensity y. With the aim to obtain a practical solution of Eq. 1, Cornell et al. [10] present the following hypothesis: 1) seismic mean annual exceedance rate, $\nu_D(y)$ can be described for a certain intensity region by the function $\nu_D(y) = ky^{-r}$; 2) the median structural demand can be estimated as $\widehat{D} = ay^b$; and 3) structural demand follows a lognormal distribution with its standard deviation of the natural logarithm [11]. Considering the above hypotheses and making some algebraic arrangements, the exceedance demand rate considering the epistemic uncertainties related to structural demand is as follows:

$$\nu_D(d) = \upsilon \left(\frac{d}{a}\right)^{1/b} \exp\left[\frac{r^2}{2b^2}\left(\sigma^2_{lnD|y}\right)\right] \tag{2}$$

where υ is the mean annual rate of exceedance associated to the minimum intensity; $(d/a)^{1/b}$ is the spectral acceleration related to a damage threshold d, $\sigma^2_{lnD|y}$ is the variance of the natural logarithm of the demand for a given seismic intensity y.

3 BUCKLING RESTRAINED BRACES

BRBs are energy dissipaters that can be replaced once they suffer damage. The BRB consists of a core plate enclosed by a restraining member to prevent buckling. An unbonded material is placed between the core plate and restraining member to ensure that the axial force carried by the core is not transferred to the restraining member. The steel core is specifically designed to resist axial forces in both tension and compression without local or global flexural failure [7]. According to [12], the lateral stiffness provides by a BRBs devices under seismic loads is as follows:

$$K_L = \frac{A_n\, E}{L} cos^2(\theta)\; k_f \tag{3}$$

where A_n is the area of the BRB core; E is the modulus of elasticity of steel; L is the total length of the element; θ is the inclination angle; k_f is a correction factor that accounts for both the ratio of the core length to the total length, and the ratio of the axial stress outside the core to the axial stress within the core of the BRB. k_f is commonly provided by BRB manufacturers. The lateral stiffness of the device can be defined as follows:

$$K_L = \frac{F_L}{\Delta_L} \tag{4}$$

where F_L is the lateral force provided by the BRBs system; Δ_L is the lateral drift of an inter-story. The shear force provided by each dissipator is given by:

$$V_{BRB} = \frac{F_L}{N_{BRBs}} \tag{5}$$

where N_{BRBs} is the number of devices in an inter-story for each analysis direction. By substituting Eq. 3 into Eq. 4, and subsequently into Eq. 6, the area of the BRB core is obtained as follows:

$$A_n = \frac{V_{BRB}\, L}{E\; cos^2(\theta)\; k_f\; \Delta_L} \tag{6}$$

4 GROUND MOTIONS

This study focuses on seismic loading as the primary environmental action. To analyze the structural response of the system, a database of 100 ground motion records from the UC44 station in Mexico City was compiled. These records include events with magnitudes between 5.0 and 8.2 that represent different seismic sources occurred over the last four decades. Figure 1 shows the linear acceleration response spectra of 100 earthquakes.

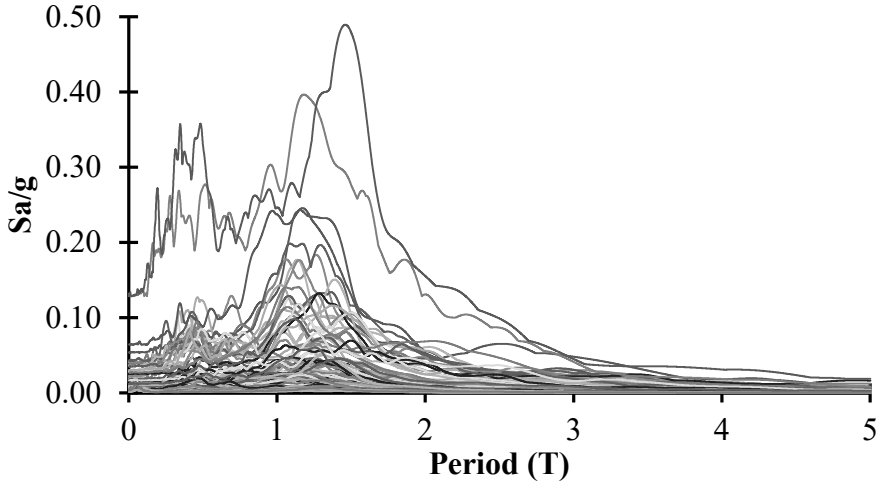

Figure 1: Linear acceleration response spectra for 100 ground motion records

5 NONLINEAR MODELING

The nonlinear response of the system is computed with the help of Ruaumoko 3D software [13]. The nonlinear structural behavior is modelled by the formation of plastic hinges at the ends of elements such as beams and columns. These hinges follow the modified Takeda hysteresis model, which is defined by the initial stiffness k_0, the unloading stiffness k_{u}, and the parameters r, α, and β. Strength degradation is incorporated using a model governed by three parameters: the ductility level at which degradation begins, the ductility level at which it ends, and the residual strength of the element. The moment-curvature relationships for each element are obtained using the Mander model for confined concrete [14] and the stress-strain relationship model for steel reinforcement [15]. The BRBs are modeled with a bilinear hysteresis rule defined by tensile and compressive yield forces, k_1, and a strain hardening factor r_1.

Mean properties are used for the analysis in which dead load is estimated by using the equation proposed by Meli [16].

$$\overline{CM} = \frac{CM}{1 + C_{vm}} \tag{7}$$

were $\overline{CM}$ is the mean value of the dead load; CM is the nominal value of dead load and C_{vm} is the variation coefficient of dead load. The mean values related to the material and geometric properties are shown in Table 1 and 2.

Table 1: Mean values of materials

Material	Nominal resistance (MPa)	Mean resistance (MPa)	Ref.
Concrete	35	36.80	[16]
Steel rebar	412	441.4	[17]

Table 2: Mean values of geometric properties

Item	Mean (m)	Ref.
Beam width	0.00254	[18]
Beam height	-0.00279	[18]
Beam bottom cover	0.0016	[18]
Beam top cover	0.0032	[18]
Column dimension	0.00159	[19]

6 CASE OF STUDY

Demand exceedance rates are estimated in a ten-story RC building hospital with BRBs. The system was designed to resist 30% of the interstory shear. The building has an irregular plant and a total height of 40m (see Figure 2). The structure is ubicated in Mexico City. The concrete compressive strength, f_c', is equal to 35 MPa and the yield strength of steel reinforcement, f_y, is equal to 412 MPa. The distribution of the dissipation system throughout the structure has been optimized to locate the BRBs in areas that contribute significantly to the structural behavior. A total of 22 BRBs per story are installed. The cross sections of beams, columns and BRBs are shown in Tables 3, 4, 5 and 6.

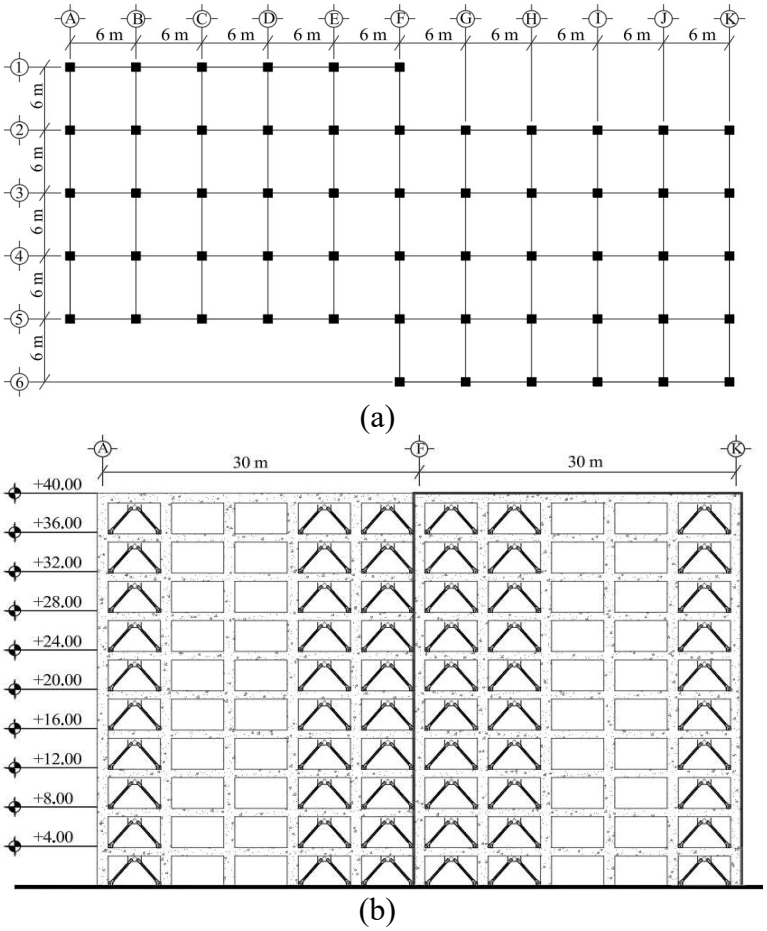

Figure 2: Structural system. (a) plant and (b) elevation.

Table 3: Beams

Story	Size (m)	Rebar at top	Rebar at bottom	Stirrups at the end
1-4	0.45 x 1.35	4#12	4#12	2#4 @ 0.15 m
5-6	0.45 x 1.30	4#12	4#12	2#4 @ 0.20 m

Table 4: Columns

Story	Size (m)	Flexural rebars	Stirrups at the end
1-4	0.95 x 1.55	14#12	2#4 @ 0.10 m
5-6	0.90 x 1.50	14#12	2#4 @ 0.10 m

Table 5: Cross-sectional area of BRBs

	X direction	Y direction
Story	Area (m^2)	Area (m^2)
1	0.0219	0.0258
2	0.0129	0.0129
3	0.0129	0.0129
4	0.0129	0.0129
5	0.0123	0.0129
6	0.0116	0.0123
7	0.0110	0.0116
8	0.0103	0.0103
9	0.0090	0.0065
10	0.0071	0.0052

6.1 Structural and nonstructural demand

The structural demand is obtained by nonlinear dynamic analysis using one hundred seismic records scaled until the failure of the system appears. Figure 3 shows the median of the structural demand at the third story. The parameters that fitted the shape of the structural demand are $a = 0.00225$ and $b = 1.36061$.

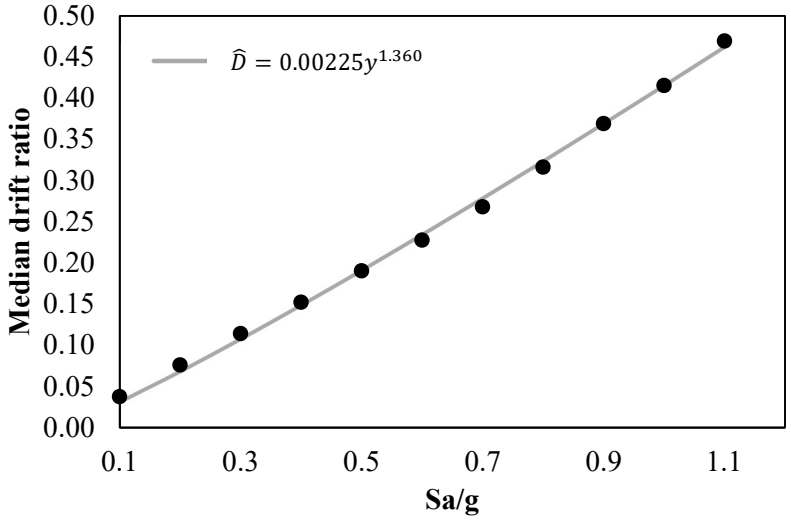

Figure 3: Median of the maximum drift ratio at the three story

The nonstructural demand is quantified in terms of the peak floor acceleration (PFA). Figure 4 illustrates the median of the nonstructural demand at the three story. The parameters that fitted the median value of the nonstructural demand are $a = 0.41454$ and $b = 1.120$.

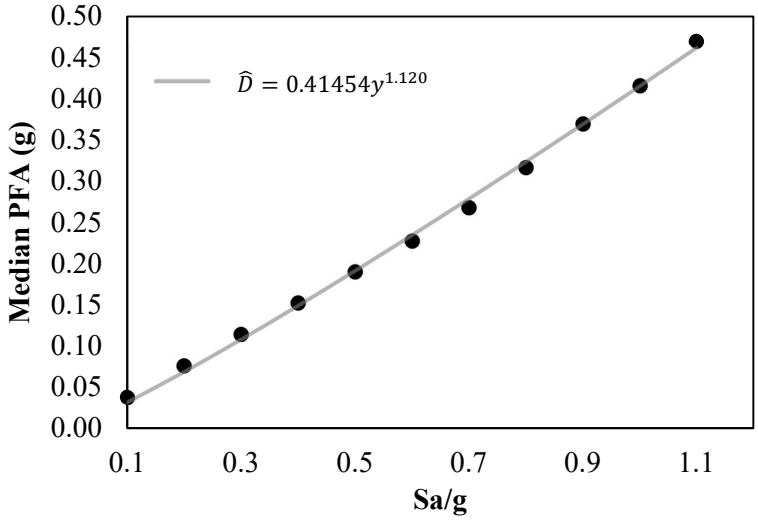

Figure 4: Median of the maximum peak floor acceleration at the three story

6.2 Seismic hazard

The seismic hazard (SH) is known, and it is associated with the fundamental period of the structure T=0.43 and an effective damping equal to 5% (see Figure 5). The seismic hazard is fitted for a region of interest with parameters equal to $k = 0.00303$ and $r = 1.79786$.

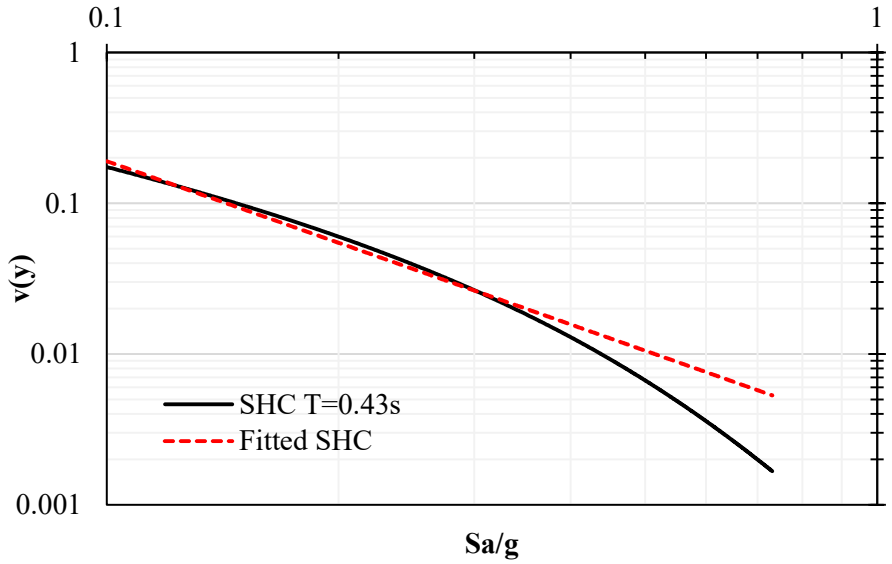

Figure 4: Seismic hazard

6.3 Structural and nonstructural fragility estimation

Fragility curves represent the probability of exceeding a certain performance threshold. The fragility function is as follows [20]:

$$P(D \geq d) = 1 - \Phi\left(\frac{\ln(d) - \ln(\bar{D}_{|y})}{\sigma_{\ln \bar{D}_{|y}}}\right) \tag{8}$$

where d is a damage or performance threshold; $\bar{D}_{i_{|y}}$ is the median value of the demand for a given seismic intensity; $\sigma_{\ln \bar{D}_{|y}}$ is the standard deviation of the natural logarithm of demand for a given seismic intensity and Φ is the normal cumulative distribution function.

Structural fragility curves are obtained for different performance levels in terms of the maximum interstory drift with values equal to 0.002, 0.004, 0.0075 and 0.0015 [21]. The fragility of nonstructural elements can be quantified in terms of interstory acceleration [22][23].

Table 6: Mean values of damage for nonstructural elements

Demand measure	Slight	Moderate	Extensive	Complete
Peak floor acceleration (g)	0.3	0.60	1.20	2.40

Figure 5 shows the seismic fragility curves. It is observed that the threshold of 0.002 presents a probability of exceedance of 0.66 at 1.1 Sa/g and for the threshold of 0.004, 0.0075 and 0.015 presents a probability of exceedance close to zero for intensities less than 0.9 Sa/g. This can be explained that the current design code of Mexico City allows the use of devices such as BRBs, damping devices, base isolation if the main structure is designed in the elastic range.

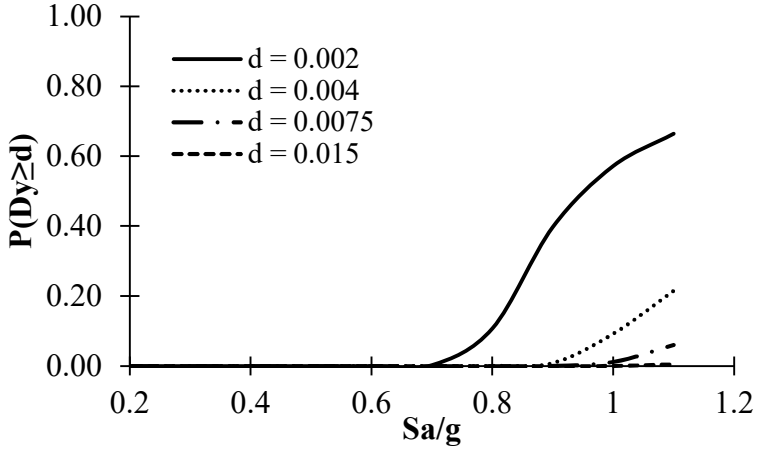

Figure 5: Seismic fragility curves at three story

The nonstructural fragility curves are obtained in terms of the peak floor acceleration considering different thresholds using the information of Table 6 (see Figure 6). It is observed that moderate and extensive damage has a probability of exceedance close to zero to intensities lower than 0.7 Sa/g and slight damage presents a probability of exceedance of 0.89 at 1.1 Sa/g.

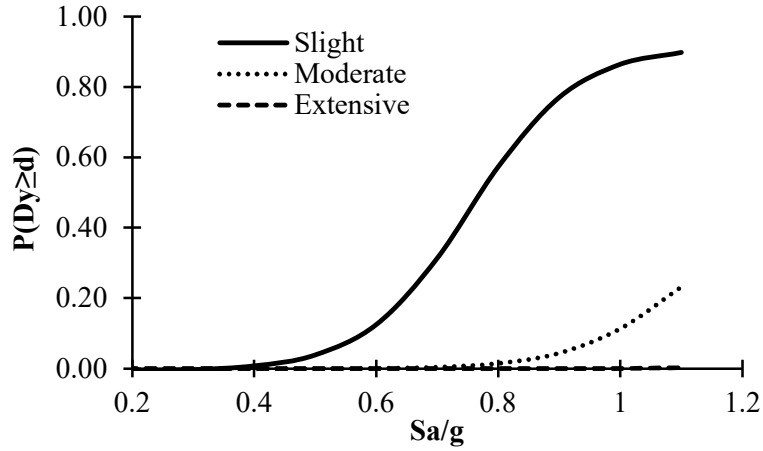

Figure 6: Seismic fragility for nonstructural elements at three story

6.4 Exceedance demand rates

Demand exceedance rates offer a probabilistic measure to know the expected structural response as the number of times per year that can be exceeded. The inverse value of the demand exceedance rate represents the return period. Figure 7 shows the demand exceedance rates in terms of the maximum drift ratio at three story. Demand exceedance rates obtained through both numerical integration (Eq. 1) and closed form expression (Eq. 2) considering different interstory drift values between 0.001 to 0.015. It is noticed that closed form expression presents differences of 8.69% regarding the numerical solution. The difference is due to the assumptions that are made to derive the close form solution. Nonstructural exceedance demand rates are estimated using peak floor acceleration with values between 0.3 to 1.2g. The difference between two approaches presents a difference of 10.11% (see Figure 8).

The results obtained with Eq. 2 indicate a return period of 646 years for the drift threshold of 0.004 associated with a mean annual exceedance rate of 0.00154. On the other hand, the performance level of 0.015 presents a mean annual exceedance rate equal to 0.000269 with a return period of 3709 years. In case of nonstructural elements, the slight damage state presents a return period of 172 years with a mean annual exceedance rate of 0.00579. The moderate damage state results with a mean annual exceedance rate of 0.00190 associated with a return period of 525 years. The extensive damage the state presents a return period of 1598 years associated with a mean annual exceedance rate of 0.000625. The non-structural components are more susceptible to present damage.

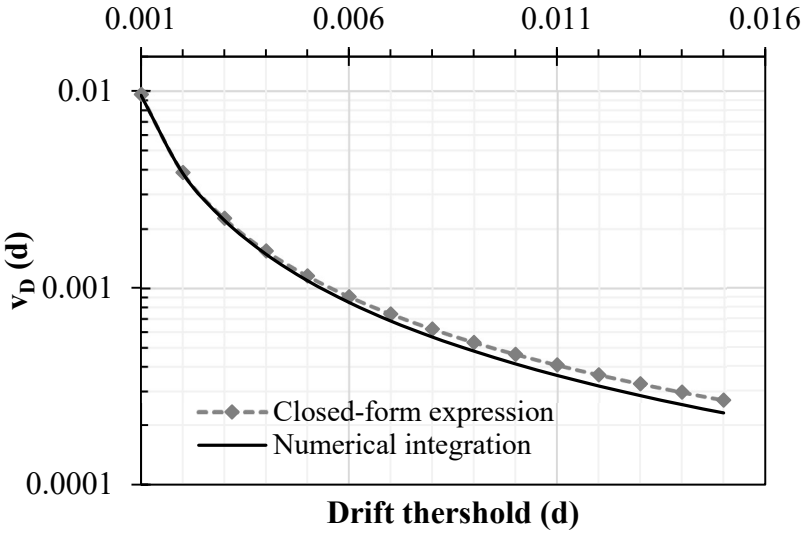

Figure 7: Exceedance demand rates at three story

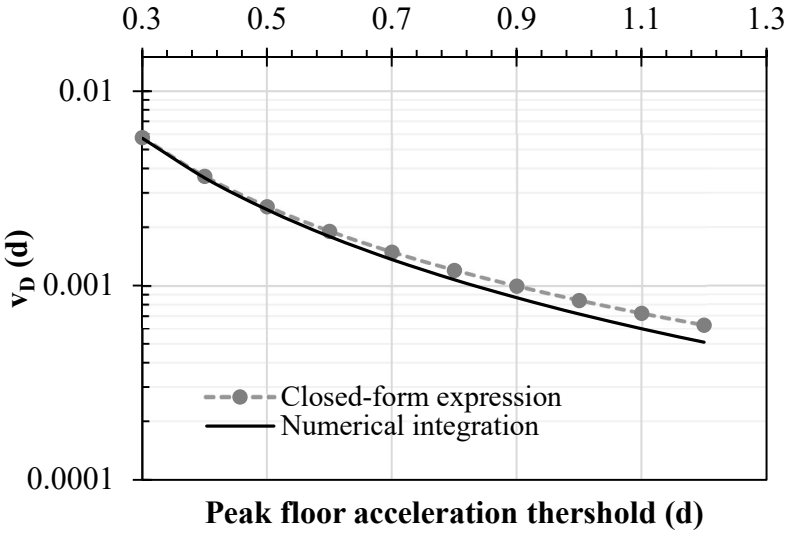

Figure 7: Exceedance demand rates for nonstructural elements at three story

7 CONCLUSIONS

Demand exceedance rates were estimated for structural and nonstructural components with the help of a reinforced concrete hospital building with BRBs exposed to seismic loads. Structural elements exhibit lower demand exceedance rates compared to nonstructural components, which demonstrate greater vulnerability to damage. This is in accordance with FEMA that emphasizes the importance of maintaining in operational levels the nonstructural components of essential facilities such as hospitals. On the other hand, structures designed with the Mexican design code must guarantee that a drift threshold of 0.004 associated with the damage limitation is not exceeded in 20 years. Based on the results, the damage limitation is exceeded after 646 years and for the nonstructural elements associated with the slight damage state is expected to be exceeded after 172 years of system construction. The demand exceedance rates estimated for both structural and nonstructural elements offer valuable insights for decision-making processes such as development of strategies to mitigate seismic risk, optimize resource allocation for retrofitting or new construction, and enhance the reliability of this kind of system to ensure their operativity under seismic events.

REFERENCES

[1] Rossetto, T., and Elnashai, A., A new analytical procedure for the derivation of displacement-based vulnerability curves for populations of RC structures. *Eng. Struct.* (2005) **27**:397–409.

[2] Rezaei Ranjbar, P., and Naderpour, H., Probabilistic evaluation of seismic resilience for typical vital buildings in terms of vulnerability curves. *Structures* (2020) **23**:314–323.

[3] Herrera, D., and Tolentino, D., Fragility Assessment of RC Bridges Exposed to Seismic Loads and Corrosion over Time. *Materials (Basel).* (2023) **16**:1100.

[4] Shooraki, M.K., Bastami, M., Abbasnejadfard, M., and Motamed, H., Development of seismic fragility curves for hospital buildings using empirical damage observations. *Int. J. Disaster Risk Reduct.* (2024) **108**:104525.

[5] Gubana, A., and Mazelli, A., Fragility curves for different intensity measures for a gravity load-designed RC hospital building: A case study. *Structures* (2023) **56**:104925.

[6] Taghavi, S., and Miranda, E., Response Assessment of Nonstructural Building Elements. *Rep. 2003/05* (2003) .

[7] Hu, J.W., Shokrgozar, H.R., Golsefidi, E.S., and Mansouri, I., Effects of Brace Configuration and Structure Height on Seismic Performance of BRBFs Based on the Collapse Fragility Analysis. *Period. Polytech. Civ. Eng.* (2020) **64**:1075–1086.

[8] Maulana, T.I., Syamsi, M.I., and Majima, R., Optimum buckling-restrained braces application to enhance seismic performance of RC frame with curtailed walls. *E3S Web Conf.* (2023) **429**:05029.

[9] Suzuki, A., Ohno, S., and Kimura, Y., Risk Assessment of Overturning of Freestanding Non-Structural Building Contents in Buckling-Restrained Braced Frames. *Buildings* (2024) **14**:3195.

[10] Cornell, C.A., Jalayer, F., Hamburger, R.O., and Foutch, D.A., Probabilistic Basis for 2000 SAC Federal Emergency Management Agency Steel Moment Frame Guidelines. *J. Struct. Eng.* (2002) **128**:526–533.

[11] E. Rosenblueth and L. Esteva, Reliability Basis for Some Mexican Codes. *ACI Symp.*

Publ. (1972) **31**:1–42.
[12] Tremblay, R., Bolduc, P., Neville, R., and DeVall, R., Seismic testing and performance of buckling-restrained bracing systems. *Can. J. Civ. Eng.* (2006) **33**:183–198.
[13] Carr, A.J., User Manual for the 3-Dimensional Version, Raumoko 3D, Vol. 3, University of Cantenbury (2007).
[14] Mander, J.B., Priestley, M.J.N., and Park, R., Theoretical Stress-Strain Model for Confined Concrete. *J. Struct. Eng.* (1988) **114**:1804–1826.
[15] Rodríguez, M., and Botero, J., Comportamiento sísmico de estructuras considerando propiedades mecánicas de aceros de refuerzo mexicanos. *Rev. Ing. Sísmica* (1995) **49**:39–50.
[16] Meli, R., and Mendoza, C.J., Reglas de verificación de calidad del concreto. *Rev. Ing.* (1991) **61**:19–24.
[17] NTC-2023, Normas Técnicas Complementarias del Reglamento de Construcciones de la Ciudad de México, *Gac. Of. La Cuid. México* (2023).
[18] Mirza, S.A., and MacGregor, J.G., Variations in Dimensions of Reinforced Concrete Members. *J. Struct. Div.* (1979) **105**:751–766.
[19] Leon H. Grant and James G. MacGregor, S.A.M., Monte Carlo Study of Strength of Concrete Columns. *ACI J. Proc.* (1978) **75**:.
[20] Tolentino, D., Márquez-Domínguez, S., and Gaxiola-Camacho, J.R., Fragility Assessment of Bridges Considering Cumulative Damage Caused by Seismic Loading. *KSCE J. Civ. Eng.* (2020) **24**:551–560.
[21] NTC-2023, Norma Técnica Complementaria Sobre Criterios Y Acciones Para El Diseño Estructural De Las Edificaciones. *Gac. Of. La Cuid. México* (2023).
[22] Federal Emergency Management Agency (FEMA), Hazus Earthquake Model Technical Manual (Hazus 5.1), in: *The Hazus Loss Estimation Methodology*, (2022) , p. 467.
[23] Hosseini, S.A., Tekantappeh, J.M., Nouri, G., and Massumi, A., Structural and non-structural fragility curves for low-rise mainshock-damaged buildings subjected to aftershocks. *Structures* (2024) **69**:107352.